A study of hyperbolicity of kinetic stochastic Galerkin system for the isentropic Euler equations with uncertainty*

Shi Jin† and Ruiwen Shu‡

September 19, 2018

Abstract

We study the fluid dynamic behavior of the stochastic Galerkin (SG) approximation to the kinetic Fokker-Planck equation with random uncertainty. While the SG system at the kinetic level is hyperbolic, its fluid dynamic limit, as the Knudsen number goes to zero and the underlying kinetic equation approaches to the uncertain isentropic Euler equations, is not necessarily hyperbolic, as will be shown in the case study fashion for various orders of the SG approximations.

1 Introduction

Hyperbolic conservation laws are one of the classical nonlinear partial differential equations with important applications from gas dynamics, shallow water, combustion, to magnetohydrodynamics. A general system of conservation laws reads

$$\partial_t U + \partial_x F(U) = 0, \tag{1.1}$$

where $t \in \mathbb{R}_{\geq 0}$ is time, and $x \in \Omega \subset \mathbb{R}$ is space, assumed to be one-dimensional for simplicity. $U(t,x) = (U_1(t,x), \ldots, U_n(t,x))^T$ is the vector of conserved quantities, and $F(U) = (F_1(U), \ldots, F_n(U))$ is the flux function, assumed to be at least C^1. The system is called *hyperbolic* if the Jacobian matrix $\nabla_U F$ is real-diagonalizable. For most models from physics in conservation forms, in particular, the compressible Euler equations in gas dynamics, the hyperbolicity condition is satisfied.

Consider the isentropic Euler equations

$$\begin{cases} \partial_t \rho + \partial_x m = 0, \\ \partial_t m + \partial_x (\rho + \dfrac{m^2}{\rho}) = 0. \end{cases} \tag{1.2}$$

*Research supported by NSF grants DMS-1522184, DMS-1819012 and DMS-1107291: RNMS KI- Net.

†School of Mathematical Sciences, Institute of Natural Sciences, MOE-LSEC and SHL-MAC, Shanghai Jiao Tong University, Shanghai 200240, China. Email: shijin-m@sjtu.edu.cn.

‡Department of Mathematics, University of Maryland, College Park, 4176 Campus Dr., College Park, MD 20742 USA. Email: rshu@cscamm.umd.edu

Here $\rho > 0$ is the density of gas, and m is the momentum. The Jacobian of $\nabla_U F$ is given by

$$J = \begin{pmatrix} 0 & 1 \\ 1 - u^2 & 2u \end{pmatrix}, \tag{1.3}$$

with $u = \frac{m}{\rho}$ being the velocity of gas. The eigenvalues of J are $u \pm 1$, and thus (1.2) is hyperbolic.

Hydrodynamic equations have two components: conservations and equations of state (or constitutive relations). While the conservation properties are basic physical properties typically satisfied for an ensemble of large number of particles, the equation of state or constitutive relations are usually *empirical*, thus inevitably contains *uncertainty*. Uncertainties also arise from initial and/or boundary data, and/or forcing or source terms, due to measurement or modeling errors. By quantifying how these uncertainties affect the behavior of the solution, one can make reliable predictions of the physical quantities modeled by the conservation laws and further calibrate or improve the models. To model the uncertainty, we introduce a random variable z lying in a random space $I_z \subset \mathbb{R}^d$ with a probability distribution $\pi(z)\,\mathrm{d}z$, and any uncertain quantity is described by its dependence on z. For example, uncertain initial data is modeled by $U_{in} = U_{in}(x, z)$. As a result, the solution U also depends on z: $U = U(t, x, z)$. The solution $U(t, x, z)$ still satisfies the same equations (1.1), but depends on an extra random parameter z.

In the last few decades, many methods have been developed for uncertainty quantification (UQ) [8, 9, 19, 28, 29], including the Monte Carlo methods, stochastic collocation (SC) methods and stochastic Galerkin (SG) methods. The Monte Carlo methods [20] solve the deterministic problem on random sample points, and then obtain statistical information by averaging. Stochastic collocation methods [1, 3, 21, 30] solve the deterministic problem on some well-chosen sample points (for example, quadrature points, or points chosen by some optimization procedure), and then compute statistical quantities by interpolation. Stochastic Galerkin methods [3, 2, 31] use a finite (K-)dimensional orthonormal basis in the random space I_z (with respect to $\pi(z)\,\mathrm{d}z$), expand any function in z in the L^2 space as a linear combination of this basis. After conducting the Galerkin projection one obtains a *deterministic* system of the K coefficients in the expansion. A popular choice of basis is the generalized polynomial chaos (gPC) basis [31], which are the orthonormal polynomials with respect to $\pi(z)\,\mathrm{d}z$.

The main advantage of the Monte Carlo methods is that it maintains a convergence order $1/2$ for any dimensional random spaces, thus it is efficient even if the dimension d is large. SC and SG methods can achieve high convergence order if the solution is sufficiently smooth in the random space, but they suffer from the 'curse of dimensionality' if d becomes large.

The Monte Carlo and SC methods are non-intrusive methods: one only needs to run the deterministic solver many times to obtain statistical information of the random solution. However, for the intrusive gPC-SG methods, the system of the gPC coefficients is a *coupled* system, which may be significantly different from the deterministic equations. One usually needs to design new numerical methods to solve it.

When applied to system of hyperbolic conservation laws (1.1), the gPC-SG method gives a system of conservation laws for the gPC coefficients which may lose the hyperbolicity, unless for special classes of systems which include:

- Symmetric conservation laws, i.e., $\nabla_U F$ is symmetric. This includes scalar conservation laws. See [10] for an example.

- Linear conservation laws, i.e., F is linear.

One example of loss of hyperbolicity is given in [5] for the Euler equations. When hyperbolicity of the gPC-SG method is lost, the initial value problem of the gPC-SG system becomes ill-posed.

One possible fix of the loss of hyperbolicty of the gPC-SG method is proposed by [24]. By using entropy variables, they write (1.1) into a symmetric form, and this symmetry can be maintained by the gPC-SG method. However, this method requires the transformation between the conservative variables U and the entropy variables in each time step and every grid point, which is very costly in general. For other efforts in this direction see [26, 23, 7].

It is well known that many hyperbolic conservation laws can be obtained as the hydrodynamic limit of kinetic equations. For example, the Euler equations are the hydrodynamic limit of the Boltzmann equation (with the hyperbolic scaling) [4], and the isentropic Euler equations (1.2) is the hydrodynamic limit of the kinetic Fokker-Planck equation [27]

$$\partial_t f + v\partial_x f = \frac{1}{\mathrm{Kn}} L_f(f), \tag{1.4}$$

where $v \in \mathbb{R}$ is the velocity variable, $f = f(t, x, v)$ is the particle distribution function, and L_f is the kinetic Fokker-Planck operator

$$L_f(g) = \partial_v(\partial_v g + (v - u)g), \quad u = \frac{m}{\rho} = \frac{\int f v \,\mathrm{d}v}{\int f \,\mathrm{d}v}. \tag{1.5}$$

Here Kn is the Knudsen number, the dimensionless particle mean free path. As $\mathrm{Kn} \to 0$, the hydrodynamic limit (1.2) is (formally) obtained.

Recently there has been a rapid progress on the gPC-SG methods for multiscale kinetic equations with uncertainty [16, 11, 14, 13, 32]. Many gPC-SG methods have the stochastic asymptotic-preserving (s-AP) property [16], which means that the method works uniformly from the kinetic regime ($\mathrm{Kn} = O(1)$) to the fluid regime ($\mathrm{Kn} << 1$), with a fixed number K of basis functions. Also, the random space regularity of the solutions for various kinetic equations have been proved, in the linear cases [12, 13, 17], and nonlinear ones [15, 18, 25]. Consequently one can even establish the spectral accuracy, uniform in Kn, of the gPC-SG methods. In the case of nonlinear kinetic equations, such results were obtained for solutions near the global Maxwellian. Note that at the kinetic level, the equation is a scalar equation, and moreover, with a linear convection, thus the gPC-SG approximations naturally preserve the hyperbolicity of the kinetic equations. Therefore, one may be curious whether the hyperbolicity of the kinetic gPC-SG system for a kinetic equation will survive in the fluid dynamic limit. If it does, then this would provide a vehicle to derive stable gPC-SG approximations for the compressible Euler equations, as in their deterministic counterparts, which is known as the *kinetic schemes* for the Euler equations [22].

In this work, we give a *counter-argument* to this. For the kinetic Fokker-Planck equation (1.4), we show that the gPC-SG system for (1.4), after taking a formal hydrodynamic limit by sending $\mathrm{Kn} \to 0$, does *not* necessarily give a hyperbolic gPC-SG approximation for (1.2). To be precise, our numerical results suggest that the gPC-SG method obtained from a kinetic approach may fail to be hyperbolic even for arbitrarily small randomness, if $K = 4$. However, for $K = 2, 3$, we prove that hyperbolicity holds under reasonable assumptions.

The paper is organized as follows: in Section 2 we introduce the gPC-SG method for the kinetic Fokker-Planck equation (1.4) with uncertainty, and formally derive its hydrodynamic

limit as the gPC-SG method for the isentropic Euler equations (1.2); in Section 3 we show that the Jacobian matrix of the gPC-SG system of (1.2), if contains imaginary eigenvalues, the imaginary part will be small if the uncertainty of ρ and m is small; in Section 4 we prove the hyperbolicity of this gPC-SG system for $K = 2, 3$ under reasonable assumptions, and provide numerical evidence suggesting that hyperbolicity may fail for arbitrarily small randomness when $K = 4$. The paper is concluded in Section 5.

2 The gPC-SG method

In this section we aim to derive a gPC-SG method for the isentropic Euler equations (1.2) with uncertainty as the hydrodynamic limit of a gPC-SG method for the kinetic Fokker-Planck equation (1.4) with uncertainty.

We start by deriving formally the hydrodynamic limit of the deterministic kinetic Fokker-Planck equation (1.4). The Fokker-Planck operator (1.5) conserves mass and momentum:

$$\int L_f(f)\,\mathrm{d}v = \int L_f(f)v\,\mathrm{d}v = 0, \quad \forall f > 0. \tag{2.1}$$

The local equilibrium of $L_f(f)$, i.e., the f with $L_f(f) = 0$, is given by the local Maxwellian

$$f = \rho M_u, \quad M_u(v) = \frac{1}{\sqrt{2\pi}} e^{-\frac{(v-u)^2}{2}}, \tag{2.2}$$

with $\rho(t,x)$ and $u(t,x)$ being the local density and bulk velocity. As $\mathrm{Kn} \to 0$ in (1.4), one can see (formally) that f is at this local equilibrium. Then by taking moments of (1.4) against $1, v$ and using (2.2), one obtains the hydrodynamic limit (1.2) with $m = \rho u$.

2.1 The gPC-SG method for (1.4)

For simplicity, we assume the random space is one-dimensional. The gPC basis associated to $\pi(z)\,\mathrm{d}z$ is denoted $\{\phi_k(z)\}_{k=1}^{\infty}$. $\phi_k(z)$ is a polynomial of degree $k-1$, satisfying the orthonormal property

$$\int \phi_j \phi_k \pi(z)\,\mathrm{d}z = \delta_{jk}. \tag{2.3}$$

We expand the solution $f(t,x,v,z)$ to (1.4) into gPC series and truncate:

$$f(t,x,v,z) = \sum_{k=1}^{\infty} f_k(t,x,v)\phi_k(z) \approx \sum_{k=1}^{K} f_k(t,x,v)\phi_k(z) := f^K(t,x,v,z). \tag{2.4}$$

Here $f_k(t,x,v)$ are the gPC coefficients, which no longer depend on the random variable z.

If one directly substitutes (2.4) into (1.4) and conduct Galerkin projection, then the term $uf = \frac{m}{\rho} f$ in the Fokker-Planck operator will become $\int \frac{m^K}{\rho^K} f^K \phi_k \pi(z)\,\mathrm{d}z$, with ρ^K, m^K defined similarly to (2.4). This term is not easy to compute numerically from the gPC coefficients $f_1, \ldots, f_K$. Instead, by conducting the gPC-SG method on the identity

$$\rho(\rho^{-1} f) = f, \tag{2.5}$$

we get an approximation

$$A(\rho)\overrightarrow{\rho^{-1} f} \approx \vec{f}, \tag{2.6}$$

where

$$\vec{f} = (f_1, \dots, f_K)^T, \tag{2.7}$$

is the vector of the gPC coefficients, and $A(\rho)$ is the multiplication matrix given by

$$A(\rho)_{ij} = \sum_{k=1}^{K} S_{ijk}\rho_k, \quad S_{ijk} = \int \phi_i\phi_j\phi_k\pi(z)\,\mathrm{d}z. \tag{2.8}$$

Notice that $A(\rho)$ is symmetric, and positive-definite if $\rho^K(z) = \sum_{k=1}^{K} \rho_k\phi_k(z) > 0$ for all z. In this case,

$$\overrightarrow{\rho^{-1}f} \approx A(\rho)^{-1}\vec{f}. \tag{2.9}$$

Similarly, we obtain

$$\overrightarrow{\frac{m}{\rho}f} \approx A(m)A(\rho)^{-1}\vec{f}. \tag{2.10}$$

Using these two approximations, we obtain the gPC system

$$\partial_t\vec{f} + v\partial_x\vec{f} = \frac{1}{\mathrm{Kn}}\vec{\mathcal{L}}_{\vec{f}}(\vec{f}). \tag{2.11}$$

Here $\vec{\mathcal{L}}$ is the vectorized Fokker-Planck operator, given by

$$\vec{\mathcal{L}}_{\vec{f}}(\vec{g}) = \partial_v(\partial_v\vec{g} + (v - \mathcal{A})\vec{g}), \quad \mathcal{A} = \mathcal{A}(\rho, m) = A(m)A(\rho)^{-1}. \tag{2.12}$$

Remark 2.1. *There is more than one way to approximate the gPC coefficients of the term $\frac{m}{\rho}f$, for example, by $A(\rho)^{-1}A(m)\vec{f}$. However, (2.12) seems to be the only consistent approximation which is easy to compute and conserves momentum (see next section for the conservation properties).*

2.2 Properties of the gPC system

(2.12) has the same conservation properties, namely,

Lemma 2.2. *(2.12) conserves mass and momentum:*

$$\int \vec{\mathcal{L}}_{\vec{f}}(\vec{f})\,\mathrm{d}v = \int \vec{\mathcal{L}}_{\vec{f}}(\vec{f})v\,\mathrm{d}v = \vec{0}. \tag{2.13}$$

Proof. It is clear that $\int \vec{\mathcal{L}}_{\vec{f}}(\vec{f})\,\mathrm{d}v = \vec{0}$. To see the second equality,

$$\int \vec{\mathcal{L}}_{\vec{f}}(\vec{f})v\,\mathrm{d}v = -\int (v - A(m)A(\rho)^{-1})\vec{f}\,\mathrm{d}v = -\vec{m} + A(m)A(\rho)^{-1}\vec{\rho} = -\vec{m} + A(m)\vec{e} = \vec{0}, \tag{2.14}$$

where $\vec{e} = (1, 0, \dots, 0)^T$. Here we used $A(\rho)^{-1}\vec{\rho} = \vec{e}$ which follows from

$$(A(\rho)\vec{e})_i = \sum_{j,k=1}^{K} S_{ijk}\rho_k\delta_{1,j} = \sum_{k=1}^{K} S_{i,1,k}\rho_k = \rho_i. \tag{2.15}$$

□

Notice that if we use $A(\rho)^{-1}A(m)$ instead of $A(m)A(\rho)^{-1}$ then the momentum conservation does not hold.

Then, similar to [14], we have the local equilibrium of $\vec{\mathcal{L}}_{\vec{f}}(\vec{f})$ given by

Lemma 2.3. *Assume $\rho^K(z) > 0$ for all z. Then $\vec{\mathcal{L}}_{\vec{f}}(\vec{f}) = \vec{0}$ implies*

$$\vec{f} = \exp(-\mathcal{A}\partial_v)(M_0\vec{\rho}), \quad M_0(v) = \frac{1}{\sqrt{2\pi}} e^{-\frac{v^2}{2}}, \tag{2.16}$$

where $\exp(-\mathcal{A}\partial_v)\vec{g}_0$ is defined as the solution at $s = 1$ to the system

$$\partial_s \vec{g} + \mathcal{A}\partial_v \vec{g} = 0, \tag{2.17}$$

with initial data $\vec{g}|_{s=0} = \vec{g}_0$.

Proof. We first show that $\exp(-\mathcal{A}\partial_v)$ is well-defined, i.e., the linear system of conservation laws (2.17) is hyperbolic. We need to show that the matrix $\mathcal{A}$ is real-diagonalizable. To see this, notice that

$$\mathcal{A} = A(m)A(\rho)^{-1} = A(\rho)^{1/2}(A(\rho)^{-1/2}A(m)A(\rho)^{-1/2})A(\rho)^{-1/2}, \tag{2.18}$$

where $A(\rho)^{1/2}$ is the square root of the symmetric positive-definite matrix $A(\rho)$. Therefore $\mathcal{A}$ is conjugate to the symmetric matrix $A(\rho)^{-1/2}A(m)A(\rho)^{-1/2}$, thus real diagonalizable.

Then, to see the local equilibrium (2.16), we use the conjugate structure of $\vec{\mathcal{L}}$:

$$\vec{\mathcal{L}}_{\vec{f}} = \exp(-\mathcal{A}\partial_v)\vec{\mathcal{L}}_0 \exp(\mathcal{A}\partial_v), \tag{2.19}$$

where $\vec{\mathcal{L}}_0(\vec{g}) = \partial_v(\partial_v\vec{g} + v\vec{g})$ is nothing but the deterministic Fokker-Planck operator acting on each component. In fact, (2.19) can be formally seen by

$$\begin{aligned}
\exp(-\mathcal{A}\partial_v)\vec{\mathcal{L}}_0\vec{g} =& \exp(-\mathcal{A}\partial_v)(\partial_v^2\vec{g} + \partial_v(v\vec{g})) \\
=& \partial_v^2 \exp(-\mathcal{A}\partial_v)\vec{g} + \partial_v \sum_{j=0}^{\infty} \frac{(-\mathcal{A})^j \partial_v^j}{j!}(v\vec{g}) \\
=& \partial_v^2 \exp(-\mathcal{A}\partial_v)\vec{g} + \partial_v \sum_{j=0}^{\infty} v\frac{(-\mathcal{A})^j \partial_v^j}{j!}\vec{g} + \partial_v \sum_{j=1}^{\infty} j\frac{(-\mathcal{A})^j \partial_v^{j-1}}{j!}\vec{g} \\
=& \partial_v^2 \exp(-\mathcal{A}\partial_v)\vec{g} + \partial_v(v\exp(-\mathcal{A}\partial_v)\vec{g}) - \partial_v(\mathcal{A}\exp(-\mathcal{A}\partial_v)\vec{g}) \\
=& \vec{\mathcal{L}}_{\vec{f}} \exp(-\mathcal{A}\partial_v)\vec{g}.
\end{aligned} \tag{2.20}$$

The null space of $\vec{\mathcal{L}}_0$ is clearly $\vec{g} = \exp(-\mathcal{A}\partial_v)(M_0\vec{C})$ where $\vec{C}$ is any constant vector. Then by taking moments, one sees $\vec{C} = \int \vec{g}\,\mathrm{d}v$. Therefore the local equilibrium (2.16) follows. □

Remark 2.4. *A rigorous proof of (2.19) can be obtained in a similar way to [14]. We omit the details.*

Using (2.16), one obtains

$$\begin{aligned}
\int \vec{f}v^2\,\mathrm{d}v = \int \exp(-\mathcal{A}\partial_v)(M_0\vec{\rho})v^2\,\mathrm{d}v = \int \sum_{j=0}^{\infty} \frac{(-\mathcal{A}\partial_v)^j}{j!}(M_0\vec{\rho})v^2\,\mathrm{d}v \\
= \sum_{j=0}^{\infty} \frac{\mathcal{A}^j}{j!}\vec{\rho}\int M_0\partial_v^j(v^2)\,\mathrm{d}v = \vec{\rho} + \mathcal{A}^2\vec{\rho},
\end{aligned} \tag{2.21}$$

where we first integrate by parts, and use the fact that only the terms with $j = 0, 2$ do not vanish. Taking moments of (2.11) and using this, one obtains the limiting fluid dynamic system

$$\begin{cases}
\partial_t\vec{\rho} + \partial_x\vec{m} = 0, \\
\partial_t\vec{m} + \partial_x(\vec{\rho} + A(m)A(\rho)^{-1}\vec{m}) = 0,
\end{cases} \tag{2.22}$$

where we used $\mathcal{A}^2\vec{\rho} = A(m)A(\rho)^{-1}\vec{m}$. This system is a consistent gPC-SG approximation of the isentropic Euler equations (1.2) since $A(m)A(\rho)^{-1}\vec{m}$ is an approximation of $\frac{m^2}{\rho}$.

(2.22) is a system of conservation laws for the $2K$ functions $\vec{\rho}$ and $\vec{m}$. The Jacobian of the flux function of (2.22) is given by the block matrix

$$J = \begin{pmatrix} 0 & I \\ I + B^{(1)} & B^{(2)} \end{pmatrix}, \tag{2.23}$$

where I stands for the identity matrix,

$$B^{(1)}_{\cdot,j} = \partial_{\rho_j}(A(m)A(\rho)^{-1}\vec{m}) = -A(m)A(\rho)^{-1}S_{\cdot,\cdot,j}A(\rho)^{-1}\vec{m}, \tag{2.24}$$

and

$$B^{(2)}_{\cdot,j} = \partial_{m_j}(A(m)A(\rho)^{-1}\vec{m}) = S_{\cdot,\cdot,j}A(\rho)^{-1}\vec{m} + A(m)A(\rho)^{-1}\vec{e}_j, \tag{2.25}$$

where the vector $(\vec{e}_j)_k = \delta_{jk}$.

3 Analysis of hyperbolicity of (2.22) for small randomness

In this section we study the eigenvalues of J, in the case when the *randomness is small*.

We assume $\vec{\rho} = (\rho_1, \epsilon\rho'_2, \ldots, \epsilon\rho'_K), \vec{m} = (m_1, \epsilon m'_2, \ldots, \epsilon m'_K)$ is such that $\rho_1 > 0$, $\rho'_2, \ldots, \rho'_K$ and $m_1, m'_2, \ldots, m'_K$ are of order $O(1)$. Here $\epsilon > 0$ is assumed to be small enough. Then we have

Theorem 3.1. *The imaginary part of any eigenvalue of J is at most $O(\epsilon^2)$.*

To prove the theorem, we start with

Lemma 3.2. *For given $\vec{\rho}, \vec{m}$, we denote the corresponding J as $J(\vec{\rho}, \vec{m})$. Then one has*

$$\mathrm{eig}(J(\vec{\rho}, \vec{m} + \alpha\vec{\rho})) = \mathrm{eig}(J(\vec{\rho}, \vec{m})) + \alpha, \tag{3.1}$$

where eig *means the eigenvalues of matrix, and the last $+\alpha$ means adding α to each eigenvalue.*

Proof. Explicit calculation shows that

$$J(\vec{\rho}, \vec{m} + \alpha\vec{\rho}) = \begin{pmatrix} 0 & I \\ I + B^{(1)} - \alpha B^{(2)} - \alpha^2 I & B^{(2)} + 2\alpha I \end{pmatrix}, \tag{3.2}$$

where $B^{(1)}, B^{(2)}$ are those in $J(\vec{\rho}, \vec{m})$. Thus

$$\begin{pmatrix} I & 0 \\ -\alpha I & I \end{pmatrix} J(\vec{\rho}, \vec{m} + \alpha\vec{\rho}) \begin{pmatrix} I & 0 \\ \alpha I & I \end{pmatrix} = \begin{pmatrix} \alpha I & I \\ I + B^{(1)} & B^{(2)} + \alpha I \end{pmatrix}, \tag{3.3}$$

i.e., $J(\vec{\rho}, \vec{m} + \alpha\vec{\rho})$ is similar to $J(\vec{\rho}, \vec{m}) + \alpha I$. Thus the conclusion follows. □

Without loss of generality, we may assume $\rho_1 = 1$. To analyze the imaginary parts of $\mathrm{eig}(J)$, one can replace $\vec{m}$ by $\vec{m} - \frac{m_1}{\rho_1}\vec{\rho}$ to make $m_1 = 0$, in view of Lemma 3.2. Since $m_1 = O(1)$, this replacement does not affect any smallness condition. From now on we will assume

$$\rho_1 = 1, \quad m_1 = 0 \tag{3.4}$$

Then we define the following matrix:

$$\tilde{J} = \begin{pmatrix} 0 & I \\ I - A(m)^2 & 2A(m) \end{pmatrix}. \tag{3.5}$$

Also define

$$P_2 = \begin{pmatrix} A(m) - I & -I \\ -A(m) - I & I \end{pmatrix}, \tag{3.6}$$

and its inverse is given by

$$P_2^{-1} = -\frac{1}{2} \begin{pmatrix} I & I \\ A(m) + I & A(m) - I \end{pmatrix}. \tag{3.7}$$

Explicit computation shows

$$\tilde{J} = P_2^{-1} \begin{pmatrix} A(m) + I & 0 \\ 0 & A(m) - I \end{pmatrix} P_2. \tag{3.8}$$

Therefore $\tilde{J}$ is conjugate to $\mathrm{diag}\{A(m) + I, A(m) - I\}$, which is real-diagonalizable since $A(m)$ is. Then we claim

Lemma 3.3. *Assume (3.4). Then*

$$J - \tilde{J} = O(\epsilon^2). \tag{3.9}$$

Proof. It suffices to check $B^{(1)} = -A(m)^2 + O(\epsilon^2)$ and $B^{(2)} = 2A(m) + O(\epsilon^2)$.

The equation for $B^{(1)}$ is clear since both $B^{(1)}$ and $-A(m)^2$ are of order $O(\epsilon^2)$.

To check the expansion for $B^{(2)}$, notice that

$$A(\rho)^{-1} = (I + \epsilon A(\rho'))^{-1} = I + O(\epsilon), \tag{3.10}$$

since $\vec{\rho'} := (0, \rho_2', \ldots, \rho_K') = O(1)$. Here we used the fact that ϵ is small enough so the spectral radius of $\epsilon A(\rho')$ is no more than $1/2$. Then

$$B^{(2)}_{\cdot,j} = S_{\cdot,\cdot,j} A(\rho)^{-1} \vec{m} + A(m) A(\rho)^{-1} \vec{e}_j = S_{\cdot,\cdot,j} \vec{m} + A(m) \vec{e}_j + O(\epsilon^2) = 2A(m)_{\cdot,j} + O(\epsilon^2), \tag{3.11}$$

since $\vec{m} = O(\epsilon)$.

□

To analyze the size of imaginary part of eigenvalues of J, we need the following lemma, which is a consequence of the Gershgorin Circle Theorem [6].

Lemma 3.4. *Suppose A, B are real matrices. Suppose A can be real-diagonalized by $PAP^{-1} = D = \mathrm{diag}\{\lambda_1, \ldots, \lambda_K\}$ with $\max(\|P\|, \|P^{-1}\|) \le C_1$, and $\|B - A\| \le C_2$. Here $\|A\| = \max_i \sum_j |a_{ij}|$. Then*

(i) Each eigenvalue η of B satisfies $|\eta - \lambda_i| \le C = C_1^2 C_2$ for some i. In particular, the imaginary part of η is at most C.

(ii) If $|\lambda_i - \lambda_j| > 2C$ for each $i < j$, then the eigenvalues $\{\eta_k\}$ of B can be arranged so that $|\eta_k - \lambda_k| \le C$, $k = 1, \ldots, K$, and B is real-diagonalizable.

Proof. First,

$$PBP^{-1} = D + P(B - A)P^{-1}. \tag{3.12}$$

Since $\|P(B-A)P^{-1}\| \le \|P\|\|B-A\|\|P^{-1}\| \le C$, it follows from the Gershgorin Circle Theorem that each eigenvalue η of B satisfies $|\eta - \lambda_i| \le C$ for some i. This proves (i).

To prove (ii), let $\eta_k(t)$ be the k-th eigenvalue of $(1-t)A+tB$, for $0 \le t \le 1$. Then each $\eta_k(t)$ is a complex-valued continuous function, with $\eta_k(0) = \lambda_k$. Also, for each fixed k, t, one has the estimate $|\eta_k(t) - \lambda_i| \le C$ for some i. Since $|\lambda_i - \lambda_j| > 2C$ for each $i < j$, the only possibility is that $|\eta_k(t) - \lambda_k| \le C$ for $0 \le t \le 1$. This shows that $|\mathrm{Re}(\eta_k(1)) - \lambda_k| \le C$, and thus $\{\eta_k(1)\}$, the eigenvalues of B, have distinct real parts. Since B is a real matrix, this implies that B is real-diagonalizable. □

Finally we prove Theorem 3.1:

Proof of Theorem 3.1. The matrix $\tilde{J}$ can be diagonalized by

$$P_1 P_2 \tilde{J} P_2^{-1} P_1^{-1} = \mathrm{diag}\{\lambda_1 + 1, \ldots, \lambda_K + 1, \lambda_1 - 1, \ldots, \lambda_K - 1\}, \tag{3.13}$$

where P_1 is an orthogonal matrix, P_2 is defined in (3.6), and $\lambda_1, \ldots, \lambda_K$ stand for the real eigenvalues of the symmetric matrix $A(m)$. This is because

$$P_2 \tilde{J} P_2^{-1} = \begin{pmatrix} A(m) + I & 0 \\ 0 & A(m) - I \end{pmatrix}, \tag{3.14}$$

is symmetric (see (3.8)), and has eigenvalues $\{\lambda_k \pm 1,\ k = 1, \ldots, K\}$. It is clear that $P_1, P_2, P_1^{-1}, P_2^{-1}$ are of order $O(1)$. Therefore the conclusion follows from Lemma 3.3 and Lemma 3.4 (i).

□

4 Analysis of hyperbolicity of (2.22) for specific values of K

In this section we analyze the hyperbolicity of (2.22) for specific values of K. We will show:

- For $K = 2$, (2.22) is hyperbolic if $\rho^K(z) = \sum_{k=1}^K \rho_k \phi_k(z) > 0$ for all $z \in I_z$ (Theorem 4.2).
- For $K = 3$, (2.22) may fail to be hyperbolic if one only assumes $\rho^K(z) > 0$ (Section 4.2.1). However, (2.22) is hyperbolic if $\rho_1 = O(1)$, $m_1 = O(1)$ and ρ_2, ρ_3, m_2, m_3 are small enough (Theorem 4.5), for some special cases of $\pi(z)$.
- For $K \ge 4$, we provide numerical evidence showing that (2.22) may fail to be hyperbolic even if $\rho_1 = O(1)$, $m_1 = O(1)$ and ρ_k, m_k, $k = 2, \ldots, K$ are small (Section 4.3).

4.1 The case $K = 2$

Lemma 4.1. *Assume $K = 2$. Define the 2*2 matrix $\Phi_{ij} = \phi_j(z_i)$, where $z_1, z_2 \in I_z$ are the two-point Gauss quadrature points (with respect to the probability measure $\pi(z)\,\mathrm{d}z$). Then for any $\vec{f} = (f_1, f_2)^T$, we have*

$$\Phi A(f) \Phi^{-1} = \mathrm{diag}\{f^K(z_1), f^K(z_2)\}. \tag{4.1}$$

Proof. We first show that the matrix Ψ defined by $\Psi_{ij} = \phi_i(z_j)w_j$, where w_1, w_2 are the quadrature weights corresponding to z_1, z_2, is the inverse of Φ. In fact,

$$(\Psi\Phi)_{ik} = \sum_j \phi_i(z_j)\phi_k(z_j)w_j = \int \phi_i\phi_k\pi(z)\,\mathrm{d}z = \delta_{ik}, \tag{4.2}$$

where the second equality is because $\phi_i\phi_k$ is a polynomial of degree at most 2, and the quadrature is exact for polynomials of degree at most 3. Similarly,

$$S_{ijk} = \int \phi_i\phi_j\phi_k\pi(z)\,\mathrm{d}z = \sum_{l=1}^{2} w_l\phi_i(z_l)\phi_j(z_l)\phi_k(z_l), \tag{4.3}$$

since $\phi_i\phi_j\phi_k$ is a polynomial of degree at most 3.

Then, denoting S_i as the matrix given by $(S_i)_{jk} = S_{ijk}$, we have

$$\begin{aligned}(\Phi S_i)_{kj} =& \sum_{l=1}^{2} \phi_l(z_k)S_{ilj} = \sum_{l,m=1}^{2} \phi_l(z_k)w_m\phi_i(z_m)\phi_l(z_m)\phi_j(z_m)\\ =& \phi_i(z_k)\phi_j(z_k) = (\mathrm{diag}\{\phi_i(z_1), \phi_i(z_2)\}\Phi)_{kj},\end{aligned} \tag{4.4}$$

where in the third equality we used $\Phi\Psi = I$. Thus

$$\Phi A(f) = \sum_{i=1}^{2} f_i\Phi S_i = \sum_{i=1}^{2} f_i\mathrm{diag}\{\phi_i(z_1), \phi_i(z_2)\}\Phi = \mathrm{diag}\{f^K(z_1), f^K(z_2)\}\Phi, \tag{4.5}$$

and the conclusion follows. □

Then it follows easily

Theorem 4.2. *Assume $K = 2$. If $\rho^K(z) > 0$ for all $z \in I_z$, then (2.22) is hyperbolic.*

Proof. We use the same notation as Lemma 4.1. Multiplying by Φ on each equation of (2.22) and using Lemma 4.1 gives

$$\begin{cases} \partial_t\tilde{\vec{\rho}} + \partial_x\tilde{\vec{m}} = 0, \\ \partial_t\tilde{\vec{m}} + \partial_x(\tilde{\vec{\rho}} + \mathrm{diag}\left\{\dfrac{m^K(z_1)}{\rho^K(z_1)}, \dfrac{m^K(z_2)}{\rho^K(z_2)}\right\}\tilde{\vec{m}}) = 0, \end{cases} \tag{4.6}$$

where $\tilde{\vec{\rho}} = \Phi\vec{\rho} = (\rho^K(z_1), \rho^K(z_2))^T$, and similar definition for $\tilde{\vec{m}}$. In other words, $(\rho^K(z_1), m^K(z_1))$ and $(\rho^K(z_2), m^K(z_2))$ satisfy the deterministic hyperbolic system (1.2). Therefore the conclusion follows from the hyperbolicity of (1.2). □

Remark 4.3. *In fact, this proof shows that for $K = 2$ the gPC system (2.22) is equivalent to a stochastic collocation method at z_1, z_2.*

4.2 The case $K = 3$

In this subsection we assume $K = 3$ and prove the hyperbolicity of (2.22) for small randomness. Same as the previous subsection, we will assume (3.4) without loss of generality.

Lemma 4.4. *Assume (3.4) and $|m_2| + |m_3| = 1$. Then there exists $c_1 > 0$ such that any two eigenvalues λ_i, λ_j of the symmetric matrix $A(m)$ satisfy $|\lambda_i - \lambda_j| \geq c_1$.*

Proof for special distributions. It is clear that all λ_i are at most $O(1)$. Therefore, it suffices to show that the discriminant of $\det(\lambda I - A(m))$ (as a cubic polynomial of λ) is away from zero. Let us write $x = m_2$, $y = m_3$, $a = S_{223}$, $b = S_{333}$ for clarity.

$$\begin{aligned}\det(\lambda I - A(m)) =& \det \begin{pmatrix} \lambda & -x & -y \\ -x & \lambda - ay & -ax \\ -y & -ax & \lambda - by \end{pmatrix} \\ =& \lambda^3 + (-(a+b)y)\lambda^2 + ((ab-1)y^2 - (a^2+1)x^2)\lambda + (-2ax^2y + ay^3 + bx^2y).\end{aligned} \tag{4.7}$$

Its discriminant is given by the degree-6 homogeneous polynomial $\mathrm{disc} = y^6 G(x^2/y^2)$. Here $G(x)$ is a degree three polynomial, given by the following in the special cases:

- When $I_z = [-1, 1]$ with the uniform distribution, ϕ_k are the normalized Legendre polynomials, and $a = \sqrt{4/5}$, $b = \sqrt{20/49}$. Then
$$G(x) = (2916/300125)(2401x^3 - 7056x^2 + 7965x + 270). \tag{4.8}$$
- When $I_z = \mathbb{R}$ with the Gaussian distribution, ϕ_k are the normalized Hermite polynomials, and $a = \sqrt{2}$, $b = \sqrt{8}$. Then
$$G(x) = 108x^3 - 162x^2 + 324x + 108. \tag{4.9}$$

One can easily verify that for both cases $G(x)$ is positive for $x > 0$. Therefore disc is always positive, if $x \neq 0$ or $y \neq 0$. Since the set $|x| + |y| = 1$ is compact and disc is continuous with respect to x and y, disc has a positive lower bound. □

Theorem 4.5. *Assume (3.4) and $|\rho_2| + |\rho_3| + |m_2| + |m_3| \le c$ with $c > 0$. If c is small enough, then J defined in (2.23) is real-diagonalizable, i.e., (2.22) is hyperbolic.*

Proof. We denote $\delta = |m_2| + |m_3|$. Then we claim

$$B^{(1)} = -A(m)^2 + O(\delta^2), \quad B^{(2)} = 2A(m) + O(c\delta), \tag{4.10}$$

where $B^{(1)}, B^{(2)}$ are the block matrices appeared in (2.23). The equation for $B^{(1)}$ is clear since both $B^{(1)}$ and $-A(m)^2$ are of order $O(\delta^2)$. To check the equation for $B^{(2)}$,

$$S_{\cdot,\cdot,j} A(\rho)^{-1} \vec{m} = S_{\cdot,\cdot,j} (I + A(\rho'))^{-1} \vec{m} = S_{\cdot,\cdot,j} \vec{m} + O(c\delta) = A(m)_{\cdot,j} + O(c\delta), \tag{4.11}$$

where $\rho' = (0, \rho_2, \rho_3)^T$, and we used $A(\rho') = O(c)$, $\vec{m} = O(\delta)$. We also used the fact that c is small enough so that $(I + A(\rho'))^{-1} = I + O(c)$.

As a consequence, $J - \tilde{J} = O(c\delta)$.

The eigenvalues of $\tilde{J}$ are $\lambda_i \pm 1$, $i = 1, 2, 3$, where λ_i are the eigenvalues of $A(m)$. By Lemma 4.4 applied on $\frac{m}{\delta}$, $|\lambda_i - \lambda_j| \ge c_1\delta$ for any $i \neq j$. Also, $\lambda_i = O(c)$, which implies that $|(\lambda_i + 1) - (\lambda_j - 1)| \ge 1$ for any i, j, if c is small enough. Therefore, if one denotes the eigenvalues of $\tilde{J}$ as $\mu_1, \dots, \mu_6$, then $|\mu_i - \mu_j| \ge c_1\delta$ for any $i \neq j$.

Now we claim that if c is small enough, then $\tilde{J}$ and J satisfy the assumptions of Lemma 3.4 (ii). In fact, we already showed in Theorem 3.1 that the transformation matrix $P = P_1 P_2$ of $\tilde{J}$ (defined in the proof of Theorem 3.1) is $C_1 = O(1)$ (following the notation in Lemma 3.4). Then we have $\|J - \tilde{J}\| = C_2 = O(c\delta)$. Therefore $C = C_1^2 C_2 = O(c\delta)$. We also have $|\mu_i - \mu_j| \ge c_1\delta$. Therefore, if we choose c small enough such that $C = O(c\delta) < c_1\delta/2$, then one has $|\mu_i - \mu_j| \ge 2C$. Then the conclusion that J is real-diagonalizable follows from Lemma 3.4 (ii). □

4.2.1 Loss of hyperbolicity for $K = 3$ with large uncertainty

We show by counterexample that for $K = 3$, even if $\rho^K(z) > 0$ for all $z \in I_z$, (2.22) may still fail to be hyperbolic if the uncertainty of m is large.

We take $I_z = [-1, 1]$ with the uniform distribution (so that $\phi_k(z)$ are the normalized Legendre polynomials). We take $\vec{\rho} = (1, -0.1076151078, -0.01061304986)^T$, $\vec{m} = (0, 4.678859141, 3.498325096)^T$. In this case one clearly has $\rho^K(z) > 0$. Numerical result shows that J has the complex eigenvalues $-2.172329053 \pm 0.009698318358i$.

4.3 The case $K \geq 4$

For $K \geq 4$, we try to find $\vec{\rho}, \vec{m}$ with (3.4) and small uncertainty (in the sense that $\epsilon := \sum_{k=2}^{K}(|\rho_k| + |m_k|)$ is small), such that $J(\vec{\rho}, \vec{m})$ has non-real eigenvalues, and we want the imaginary part of non-real eigenvalues as large as possible. We take $I_z = [-1, 1]$ with the uniform distribution (so that $\phi_k(z)$ are the normalized Legendre polynomials). The algorithm for finding such $\vec{\rho}, \vec{m}$ and the numerical parameters are described in Appendix.

We take $K = 4, 5, 6$ and various values of size of randomness ϵ. For each K, we plot the maximal imaginary part of eigenvalues of J found by the algorithm (the variable *maximag* in the algorithm) versus ϵ, see Figure 1. One can clearly see that for each K, *maximag* is proportional to ϵ^3. In particular, this result strongly suggests that there are examples for which J has non-real eigenvalues for arbitrarily small size of randomness. Also, this result suggests that Theorem 3.1 may not be sharp: the sharp estimate could be $O(\epsilon^3)$.

5 Conclusion

In this paper, we study the fluid dynamic behavior of the stochastic Galerkin system to the kinetic Fokker-Planck (FP) equation with random uncertainty. As the Knudsen number goes to zero, the FP system approaches to the isentropic Euler system with uncertainty. For various orders of the Stochastic Galerkin (SG) system for the FP, we show that their fluid dynamic limits, which give rise to SG systems to the Euler equations, are not necessarily hyperbolic. Thus one cannot expect to derive kinetic SG system to the isentropic Euler equations with uncertainty from the kinetic approximation, in contrast to the deterministic case where kinetic approximations provide a robust mechanism to derive kinetic schemes for the Euler equations.

Our analysis was carried out in the case study fashion, for various orders of the SG approximation. So far there has been no general theory for general order of the SG approximation. It will be interesting to develop a more general theory for the problem. It will also be interesting to study the problem for the full Euler equations as the fluid dynamic limit of the Boltzmann equation.

Acknowledgement

We thank Prof. Pierre Degond for stimulating discussions and encouragement for this work.

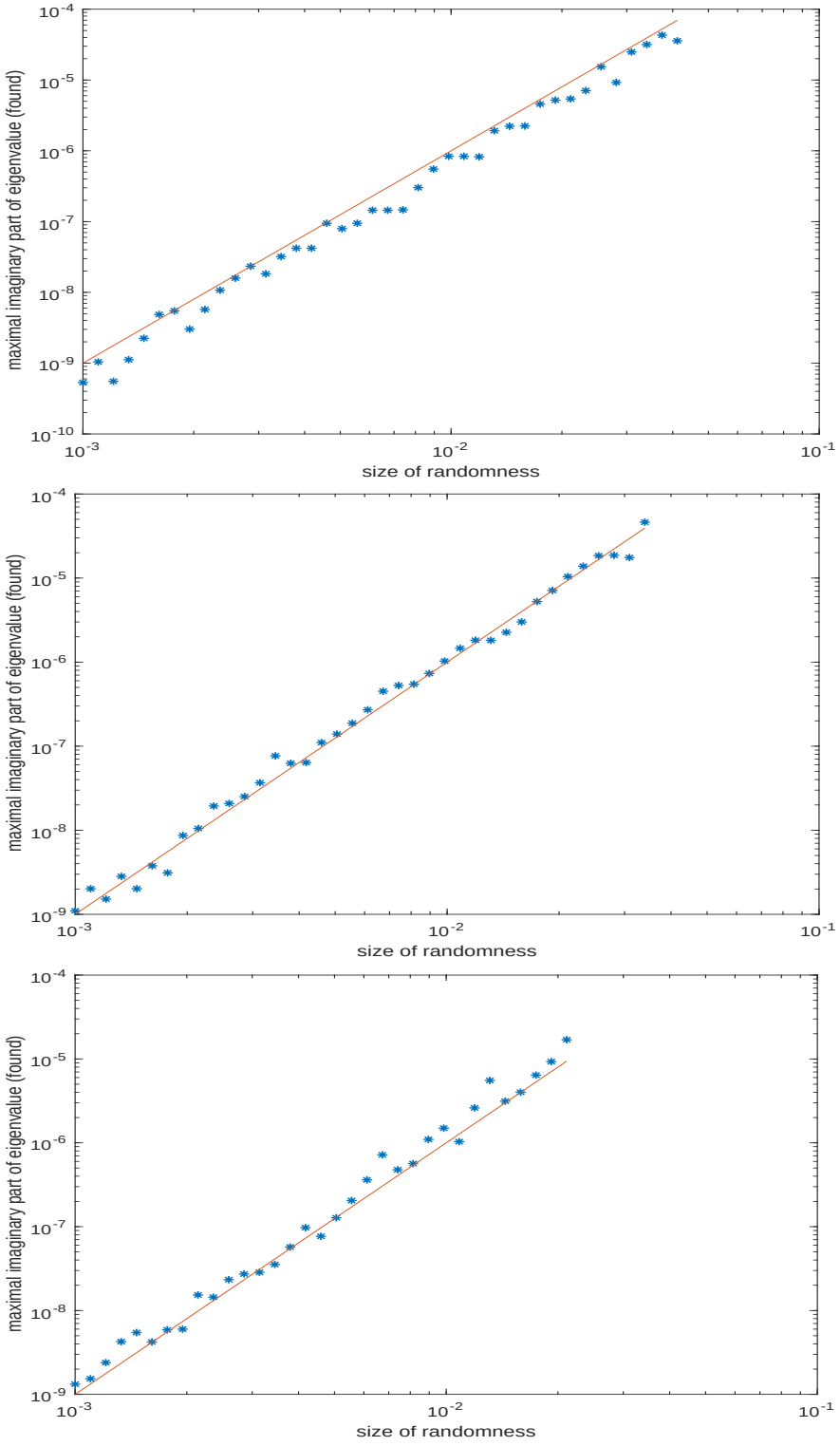

Figure 1: Maximal imaginary part of eigenvalues of J (found by Algorithm 5) versus ϵ. From top to bottom: $K = 4, 5, 6$. Horizontal axis: the size of randomness ϵ. Blue asterisks: maximal imaginary part of eigenvalues of J (found by Algorithm 5). Red line: slope= 3.

Appendix: the algorithm for finding J with non-real eigenvalues

We use the following algorithm to find J with non-real eigenvalues: for a randomly chosen $(\vec{\rho}, \vec{m})$, we try to adjust $(\vec{\rho}, \vec{m})$ to decrease the minimum distance of two distinct real eigenvalues of J as much as possible. This procedure drives J to have multiple eigenvalues, and one expects a small perturbation may make J have non-real eigenvalues, in case there are no obstruction for the eigenvalues of being non-real. Then we try to adjust $(\vec{\rho}, \vec{m})$ to increase the imaginary parts of non-real eigenvalues.

Here we provide the code for the algorithm used in Section 4.3 to find J with non-real eigenvalues. It looks for $\vec{\rho}, \vec{m}$ such that the size of randomness, measured by $\sum_{k=2}^{K}(|\rho_k| + |m_k|)$, is equal to a given $\epsilon > 0$. We need three numerical parameters n_{trial}, n_{iter1}, and n_{iter2}, whose meanings are explained as follows: for each randomly chosen $(\vec{\rho}, \vec{m})$, we try n_{iter1} times to adjust it in order to decrease the minimum distance of two distinct real eigenvalues of J. In case we find $(\vec{\rho}, \vec{m})$ such that J has non-real eigenvalues, we then try n_{iter2} times to adjust it in order to increase the imaginary parts of non-real eigenvalues. The whole procedure is repeated n_{trial} times and the largest imaginary part of non-real eigenvalues (the variable $maximag$) is reported. In all the numerical results, we take the numerical parameters $n_{trial} = 100$ and $n_{iter1} = n_{iter2} = 1000$.

References

[1] I. Babuska, F. Nobile, and R. Tempone. A stochastic collocation method for elliptic partial differential equations with random input data. *SIAM Journal on Numerical Analysis*, 45(3):1005–1034, 2007.

[2] I. Babuska, R. Tempone, and G. E. Zouraris. Galerkin finite element approximations of stochastic elliptic partial differential equations. *SIAM Journal on Numerical Analysis*, 42(2):800–825, 2004.

[3] J. Back, F. Nobile, L. Tamellini, and R. Tempone. Stochastic spectral Galerkin and collocation methods for PDEs with random coefficients: a numerical comparison. In E. M. Rønquist J. S. Hesthaven, editor, *Spectral and High Order Methods for Partial Differential Equations*. Springer-Verlag Berlin Heidelberg, 2011.

[4] C. Bardos, F. Golse, and D. Levermore. Fluid dynamics limits of kinetic equations. I. formal derivations. *J. Stat. Phys.*, 63(1-2):323–344, 1991.

[5] B. Despres, G. Poette, and D. Lucor. Robust uncertainty propagation in systems of conservation laws with the entropy closure method. In *Uncertainty Quantification in Computational Fluid Dynamics*. Springer, 2013.

[6] S. Gershgorin. Über die abgrenzung der eigenwerte einer matrix. *Izv. Akad. Nauk. USSR Otd. Fiz.-Mat. Nauk*, 6:749–754, 1931.

[7] Stephan Gerster, Michael Herty, and Aleksey Sikstel. Hyperbolic stochastic Galerkin formulation for the p-system.

Algorithm 1 Look for $\vec{\rho}, \vec{m}$ such that J has large non-real eigenvalues

Require: $\epsilon > 0$, n_{trial}, n_{iter1}, $n_{iter2} \in \mathbb{Z}_{>0}$

Ensure: Print $\vec{\rho}^{max}, \vec{m}^{max}, maximag$ such that $\rho_1 = 1, m_1 = 0, \sum_{k=2}^{K}(|\rho_k| + |m_k|) = \epsilon$, and $\text{eig}(J(\vec{\rho}^{max}, \vec{m}^{max}))$ has a complex eigenvalue with imaginary part $maximag > 0$, or print 'Did not found'.

$maximag \leftarrow 0$
for $i_{trial} = 1 : n_{trial}$ **do**
  $\rho_1 \leftarrow 1, \quad m_1 \leftarrow 0$
  Randomly generate ρ_k, m_k, $k = 2, \ldots, K$ such that $\sum_{k=2}^{K}(|\rho_k| + |m_k|) = \epsilon$
  $eigJ \leftarrow \text{eig}(J(\vec{\rho}, \vec{m}))$
  $ind \leftarrow \min\{|\lambda_1 - \lambda_2| : \lambda_1, \lambda_2 \in eigJ, \lambda_1 \neq \lambda_2\}$
  for $i_{iter1} = 1 : n_{iter1}$ **do**
    if not isreal($eigJ$) **then**
      break
    end if
    Perturb ρ_k, m_k, $k = 2, \ldots, K$ into ρ_k^1, m_k^1 randomly, with size of perturbation ind, such that they do not change sign, and $\sum_{k=2}^{K}(|\rho_k| + |m_k|) = \epsilon$ is kept the same.
    $eigJ^1 \leftarrow \text{eig}(J(\vec{\rho}^1, \vec{m}^1))$
    $ind^1 \leftarrow \min\{|\lambda_1 - \lambda_2| : \lambda_1, \lambda_2 \in eigJ^1, \lambda_1 \neq \lambda_2\}$
    if not isreal($eigJ^1$) or $ind^1 < ind$ **then**
      $\vec{\rho} \leftarrow \vec{\rho}^1, \quad \vec{m} \leftarrow \vec{m}^1, \quad eigJ \leftarrow eigJ^1, \quad ind \leftarrow ind^1$
    end if
  end for
  if isreal($eigJ$) **then**
    continue
  end if
  $ind \leftarrow \max\{\text{Im}(\lambda) : \lambda \in eigJ\}$
  for $i_{iter2} = 1 : n_{iter2}$ **do**
    Perturb ρ_k, m_k, $k = 2, \ldots, K$ into ρ_k^1, m_k^1 randomly, with size of perturbation ind, such that they do not change sign, and $\sum_{k=2}^{K}(|\rho_k| + |m_k|) = \epsilon$ is kept the same.
    $eigJ^1 \leftarrow \text{eig}(J(\vec{\rho}^1, \vec{m}^1))$
    if isreal($eigJ^1$) **then**
      $ind^1 \leftarrow 0$
    else
      $ind^1 \leftarrow \max\{\text{Im}(\lambda) : \lambda \in eigJ^1\}$
    end if
    if $ind^1 > ind$ **then**
      $\vec{\rho} \leftarrow \vec{\rho}^1, \quad \vec{m} \leftarrow \vec{m}^1, \quad eigJ \leftarrow eigJ^1, \quad ind \leftarrow ind^1$
    end if
  end for
  if $ind > maximag$ **then**
    $\vec{\rho}^{max} \leftarrow \vec{\rho}, \quad \vec{m}^{max} \leftarrow \vec{m}, \quad maximag \leftarrow ind$
  end if
end for
if $maximag > 0$ **then**
  print $\vec{\rho}^{max}, \vec{m}^{max}, maximag$
else
  print 'Did not found'
end if

[8] R. G. Ghanem and P. D. Spanos. *Stochastic Finite Elements: A Spectral Approach*. Springer-Verlag, New York, 1991.

[9] Max D. Gunzburger, Clayton G. Webster, and Guannan Zhang. Stochastic finite element methods for partial differential equations with random input data. *Acta Numer.*, 23:521–650, 2014.

[10] J. Hu, S. Jin, and D. Xiu. A stochastic Galerkin method for Hamilton-Jacobi equations with uncertainty. *SIAM J. Sci. Comput.*, 37:A2246–A2269, 2015.

[11] Jingwei Hu and Shi Jin. A stochastic Galerkin method for the Boltzmann equation with uncertainty. *Journal of Computational Physics*, 315:150–168, 2016.

[12] S. Jin, J.-G. Liu, and Z. Ma. Uniform spectral convergence of the stochastic Galerkin method for the linear transport equations with random inputs in diffusive regime and a micro-macro decomposition based asymptotic preserving method. *Research in Math. Sci.*, 4:15, 2017.

[13] S. Jin and L. Liu. An asymptotic-preserving stochastic Galerkin method for the semiconductor Boltzmann equation with random inputs and diffusive scalings. *SIAM Multiscale Modeling and Simulation*, 15:157–183, 2017.

[14] S. Jin and R. Shu. A stochastic asymptotic-preserving scheme for a kinetic-fluid model for disperse two-phase flows with uncertainty. *J. Comput. Phys.*, 335:905–924, 2017.

[15] S. Jin and Y. Zhu. Hypocoercivity and uniform regularity for the Vlasov-Poisson-Fokker-Planck system with uncertainty and multiple scales. *SIAM J. Math. Anal.*, to appear.

[16] Shi Jin, Dongbin Xiu, and Xueyu Zhu. Asymptotic-preserving methods for hyperbolic and transport equations with random inputs and diffusive scalings. *J. Comput. Phys.*, 289:35–52, 2015.

[17] Q. Li and L. Wang. Uniform regularity for linear kinetic equations with random input based on hypocoercivity. *SIAM Uncertainty Quantification*, accepted.

[18] Liu Liu and Shi Jin. Hypocoercivity based sensitivity analysis and spectral convergence of the stochastic Galerkin approximation to collisional kinetic equations with multiple scales and random inputs. *Multiscale Modeling & Simulation*, 16(3):1085–1114, 2018.

[19] O. P. Le Maître and O. M. Knio. *Spectral Methods for Uncertainty Quantification, Scientific Computation, with Applications to Computational Fluid Dynamics*. Springer, New York, 2010.

[20] H. Niederreiter, P. Hellekalek, G. Larcher, and P. Zinterhof. *Monte Carlo and Quasi-Monte Carlo Methods 1996*. Springer-Verlag, 1998.

[21] F. Nobile, R. Tempone, and C. G. Webster. A sparse grid stochastic collocation method for partial differential equations with random input data. *SIAM J. Numer. Anal.*, 46(5):2309–2345, 2008.

[22] Benoıt Perthame. Second-order Boltzmann schemes for compressible Euler equations in one and two space dimensions. *SIAM Journal on Numerical Analysis*, 29(1):1–19, 1992.

[23] Per Pettersson, Gianluca Iaccarino, and Jan Nordström. A stochastic Galerkin method for the Euler equations with Roe variable transformation. *Journal of Computational Physics*, 257:481–500, 2014.

[24] G. Poette, B. Despres, and D. Lucor. Uncertainty quantification for systems of conservation laws. *J. Comput. Phys.*, 228:2443–2467, 2009.

[25] R. Shu and S. Jin. Uniform regularity in the random space and spectral accuracy of the stochastic Galerkin method for a kinetic-fluid two-phase flow model with random initial inputs in the light particle regime. *Math. Model Num. Anal.*, to appear.

[26] Julie Tryoen, Olivier Le Maitre, Michael Ndjinga, and Alexandre Ern. Roe solver with entropy corrector for uncertain hyperbolic systems. *Journal of computational and applied mathematics*, 235(2):491–506, 2010.

[27] C. Villani. A review of mathematical topics in collisional kinetic theory. In S. Friedlander and D. Serre, editors, *Handbook of Mathematical Fluid Mechanics*, volume I, pages 71–305. North-Holland, 2002.

[28] D. Xiu. Fast numerical methods for stochastic computations: a review. *Communications in Computational Physics*, 5(2-4):242–272, 2009.

[29] D. Xiu. *Numerical Methods for Stochastic Computation*. Princeton University Press, Princeton, New Jersey, 2010.

[30] D. Xiu and J. S. Hesthaven. High-order collocation methods for differential equations with random inputs. *SIAM J. Sci. Comput.*, 27(3):1118–1139, 2005.

[31] D. Xiu and G. E. Karniadakis. The Wiener-Askey polynomial chaos for stochastic differential equations. *SIAM J. Sci. Comput.*, 24(2):619–644, 2002.

[32] Y. Zhu and S. Jin. The Vlasov-Poisson-Fokker-Planck system with uncertainty and a one-dimensional asymptotic-preserving method. *SIAM Multiscale Model. and Simul.*, 15:1502–1529, 2017.